ARCHIVES
Of
FOUNDRY ENGINEERING

ISSN (1897-3310)
Volume 11
Special Issue
2/2011
13–18

3/2

Published quarterly as the organ of the Foundry Commission of the Polish Academy of Sciences

Numerical analysis of stress fields generated by quenching process

A. Bokota[*a], T. Domański[b], L. Sowa[b]
Institute of Computer and Information Sciences[a], Institute of Mechanics and Machine Design[b]
Czestochowa University of Technology 42-200 Częstochowa, 73 Dąbrowskiego str., Poland
[*]Corresponding author: e-mail: adam.bokota@icis.pcz.pl

Received 11.04.2011; Approved for print on: 26.04.2011

Abstract

In work the presented numerical models of tool steel hardening processes take into account mechanical phenomena generated by thermal phenomena and phase transformations. In the model of mechanical phenomena, apart from thermal, plastic and structural strain, also transformations plasticity was taken into account. The stress and strain fields are obtained using the solution of the Finite Elements Method of the equilibrium equation in rate form. The thermophysical constants occurring in constitutive relation depend on temperature and phase composite. For determination of plastic strain the Huber-Misses condition with isotropic strengthening was applied whereas for determination of transformation plasticity a modified Leblond model was used. In order to evaluate the quality and usefulness of the presented models a numerical analysis of stresses and strains associated hardening process of a fang lathe of cone shaped made of tool steel was carried out.

Keywords: Quenching, stresses, transformations plasticity, numerical simulation, tool steel

1. Introduction

Today an intense development of numerical methods supporting designing or improvement of already existing technological processes are observed. The technologies mentioned above include also steel thermal processing comprising hardening. Efforts involving thermal processing numerical models aim to encompass an increasing number of input parameters of such a process [1-4].

Predicting of final properties of the element undergoing hardening is possible after determination, first of all, thermal phenomena, phase transitions and mechanical circumstances in the numerical model [1-5] (Fig. 1).

The results of the numerical simulations of the phenomena mentioned above are dependent on the precision in calculation of the instantaneous temperature and phase fractions, the latter significantly affecting the instantaneous and residual stresses. Therefore accuracy of the solid-state phase transformations model for each steel grade is very important here.

In the model of phase transformations take advantage of diagrams of continuous heating (CHT) and cooling (CCT) [6,7].

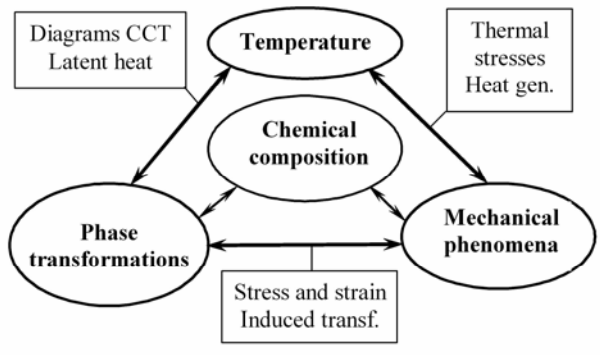

Fig. 1. Scheme of correlation of the hardening phenomena

Numerical simulations of steel thermal processing must be referred to in the transformation strains models [8-10]. This phenomenon causes metal irregular plastic flow which is observed during solid-state phase transformations especially during the decomposition of austenite into martensite. Literature presents two separate transformation strains mechanisms, one proposed by Greenwood and Johnson and another one – by Magee [5,8,11]. The Greenwood–Johnson model assumes that transformation plasticity are microplasticity occurring at the weaker austenite phase caused by the difference of specific volume between the phases. In the Magee interpretation (for the martensite transformation) it is a result of a change of the orientation of the newly-created martensite plates caused by external loading. Priorities of these mechanisms depend on the material and transformation type. The Greenwood–Johnson model prevails in diffusion transformations, but also in the transforamatins of bainite and martensite where the specific volume differs between the phases.

A modified Leblond's model was applied in the study to evaluate the transformation plasticity [8]. Literature mentions other models of evaluation of transformation strains [1,3,5]. Nethertheless, the Leblond model (based upon the Greenwood–Johnson mechanism) comprises all transformations and is the most popular model applied by researchers dealing with thermal process modeling. In the study the CCT diagram-based models are proposed.

Finite Element Method is the method most frequently used to implement numerical algorithms. This method enables to easily include in the analysis both non-linearity and non-homogeneity of the material [1,12].

2. Temperature fields and phase fractions

Temperature field are obtain with solved of transient heat equation (Fourier equation) with source unit.

Superficial heating investigation in model by boundary conditions Neumann (heat flux q_n), however cooling are modelling by boundary conditions Newton with depend on temperature coefficient of heat transfer:

$$-\lambda\left.\frac{\partial T}{\partial n}\right|_{\Gamma} = q_n = \alpha(T)\left(T\big|_{\Gamma} - T_{\infty}\right) \tag{1}$$

and also radiation through overall heat transfer coefficient was taken into account:

$$-\lambda\left.\frac{\partial T}{\partial n}\right|_{\Gamma} = q_n = \alpha_0\sqrt[3]{T\big|_{\Gamma} - T_{\infty}}\left(T\big|_{\Gamma} - T_{\infty}\right) \tag{2}$$

where: $\alpha(T)$ is heat transfer coefficient, α_0 is heat transfer coefficient experimental determine, Γ is surface external, from witch is transfer heat, T_∞ is temperature of medium ambient.

In both case the phase fractions transformed during continuous heating (austenite) is calculated using the Johnson-Mehl and Avrami formula or modified Koistinen and Marburger formula (in relations on rate of heating) [2,3,5]. Pearlite and bainite fraction are determine by Johnson-Mehl and Avrami formula. The nascent fraction of martensite is calculated using the Koistinen and Marburger formula or modified Koistinen and Marburger formula [1-3,6,12,14-16]. The methods for calculation of the fractions of the phases created referred to above were used for carbon tool steel. On the basis of the analysis of simulation and dilatometric curves the values of the thermal expansion coefficient and isotropic structural deformations of each structural component were specified [6,17].

The problem solved by Finite Elements Method [12].

3. Stresses and strains

In the model of mechanical phenomena the equations of equilibrium and constitutive relationship accept in rate form [4,7,13,18]:

$$\nabla\dot{\boldsymbol{\sigma}}(x_\alpha,t) = \mathbf{0},\ \dot{\boldsymbol{\sigma}} = \dot{\boldsymbol{\sigma}}^T,\ \dot{\boldsymbol{\sigma}} = \mathbf{D}\circ\dot{\boldsymbol{\varepsilon}}^{\mathrm{e}} + \dot{\mathbf{D}}\circ\boldsymbol{\varepsilon}^{\mathrm{e}} \tag{3}$$

where: $\boldsymbol{\sigma}=\boldsymbol{\sigma}(\sigma_{\alpha\beta})$ is stress tensor, $\mathbf{D}=\mathbf{D}(\nu,E)$ is tensor of material constant (isotropic material), ν is Poisson coefficient, $E= E(T)$ is Young's modulus depend on temperature, whereas $\boldsymbol{\varepsilon}^{\mathrm{e}}$ is tensor of elastic strain.

Assumption additives of strains, total strain in environment of considered point are equal:

$$\boldsymbol{\varepsilon} = \boldsymbol{\varepsilon}^{e} + \boldsymbol{\varepsilon}^{Tph} + \boldsymbol{\varepsilon}^{tp} + \boldsymbol{\varepsilon}^{p} \tag{4}$$

where: $\boldsymbol{\varepsilon}^{Tph}$ are isotropic temperature and structural strain, $\boldsymbol{\varepsilon}^{tp}$ are transformations plasticity, whereas $\boldsymbol{\varepsilon}^{p}$ are plastic strain.

To mark plastic strain the non-isothermal plastic law of flow with the isotropic strengthening and condition plasticity of Huber-Misses were used. Plasticize stress is depending on phase fraction, temperature and plastic strain

$$Y\left(T,\eta,\varepsilon_{ef}^{\mathrm{p}}\right) = Y_0\left(T,\eta\right) + Y_H\left(T,\varepsilon_{ef}^{\mathrm{p}}\right) \tag{5}$$

where: $Y_0 = Y_0(T,\eta)$ is a yield points of material dependent on the temperature and phase fraction (see Fig. 3), $Y_H = Y_H\left(T,\varepsilon_{ef}^{p}\right)$ is a surplus of the stress resulting from the material hardening.

Transformations plasticity estimate are by Leblond formula, supplement of decrease function ($1-\eta_{(.)}$) propose by authors in work [8,14]:

$$\dot{\boldsymbol{\varepsilon}}^{\mathrm{tp}} = \begin{cases} 0, & \eta_k \le 0.03, \\ -3\sum_{k=2}^{k=5}\left(1-\eta_k\right)\varepsilon_{1\_k}^{ph}\dfrac{\mathbf{S}}{Y_1}\ln\left(\eta_k\right)\dot{\eta}_k, & \eta_k \ge 0.03 \end{cases} \tag{6}$$

where: $3\varepsilon_{1\_k}^{ph}$ are volumetric structural strains when the material is transformed from the initial phase „1" into the k-phase, $\mathbf{S}$ is the deviator of stress tensor, Y_1 is plasticize stress of initial phase (austenite), beside,

$$Y_1 = Y_1^0 + \kappa^Y \varepsilon_{ef}^{tp} \tag{7}$$

Y_1^0 is yield points of initial phase, $\kappa^Y = \kappa^Y(T)$ is hardening modulus of material, a ε_{ef}^{tp} is effective transformations strain.

Equations of equilibrium (3) solve by Finite Elements Method, and in range plasticization of material, iterative process modified method Newton-Raphson are perform [12].

4. Example simulation of hardening element of the machine

In the simulations of hardening was subject the fang lathe of cone (axisymmetrical object) made of tool steel. The shape and dimensions considered object was presented on the figure 2.

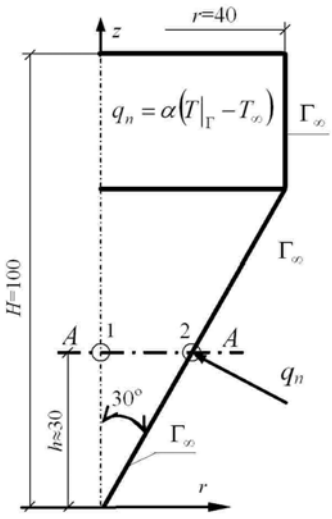

Fig. 2. Form and dimensions of the hardening object

The superficial heating (surface hardening) the section of side surface of cone was modelling Neumann boundary conditions taken Gauss distributions of heating source:

$$q_n = \frac{Q}{2\pi r^2} \exp\left(-\frac{1}{2r^2} \left(\frac{z-h}{\cos\alpha} \right)^2 \right) \tag{8}$$

The peak value of heating source established on Q=3500 W, radius r=15 mm, angle α=30° (Fig. 2). The cooling of boundary contact with air was modelled boundary conditions (2) taking α_0=30 W/(m^{2}K) [13]. It was assumed that the initial structure of pearlite. The thermophysical values occurrence in conductivity equations (λ,C) was taken constant, averages values from passed in work data [3,4] The initial temperature and ambient temperature was assumed equal 300 K.

In the modelling of mechanical phenomena the Young's and tangential modulus (E i E^t) was depend on temperature however the yield point (Y_0) on temperature and phase fractions. The values approximated of square functions (Fig. 3) assumed: Young's and tangential modulus 2.2×10^5 and 1.1×10^4 [MPa] (E_t=0.05E), yield points 150, 400, 800 and 270 [MPa] suitably for austenite, bainite, martensite and pearlite, in temperature 300 K. In temperature 1700 K Young's and tangential modulus average 100 and 5 [MPa] siutable, however yield points are equal 5 [MPa].

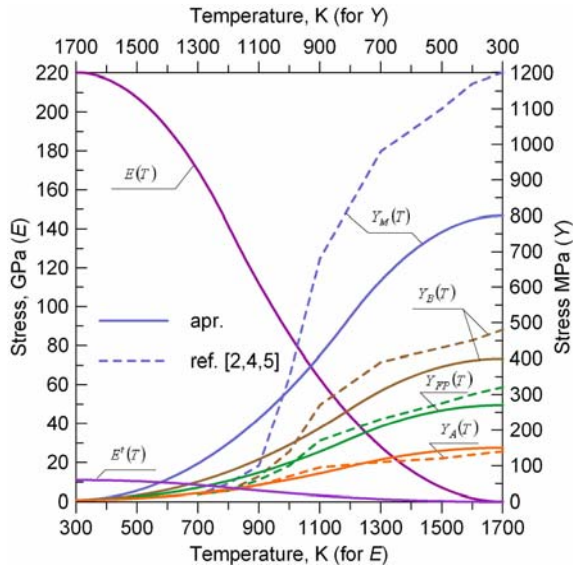

Fig. 3. Diagrams of functions $E(T)$, $E^t(T)$ and $Y_0(T,\eta)$

Young's and tangential modulus and yield point for pearlite in temperature 300 K establish on the basis own research estimated tension graph for considered steel. The others values assumed on the literature [2,4,19]. Yield point for martensite assumed as average values presented through authors of works [2,4].

The heating performed to the moment of cross maximal temperature 1500 K in environment of heat source. Provide this obtain requirements austenite zone in parts conic fang lathe [17].

The cooling simulated by flux results from the difference of temperature among side surface and cooling medium (Newton condition). The temperature of cooling medium is equal 300 K. The coefficient of thermal conductivity was equal α=4000 [W/(m^{2}K)] (cooling in fluid layer [20]). The cooling performed to obtain by object ambient temperature, and final stresses that residual stresses.

Obtained results of simulations were presented on following figures. The part of results along the radius (r) in cross section A-A and in distinguish points of cross sections (Fig. 2). These are the depositions of bainite and martensite, instantaneous and residual stresses.

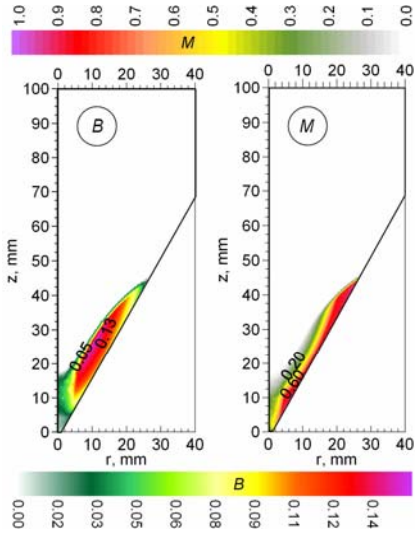

Fig. 4. Zones: bainite a) and martensite b) after quenching

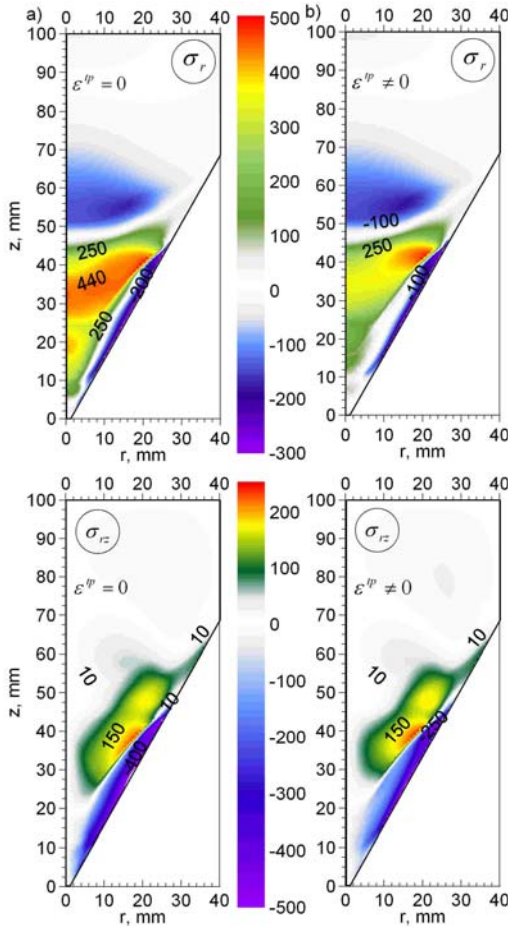

Fig. 5. Distributions of radial and tangential stresses: without a) and with b) transformations plasticity

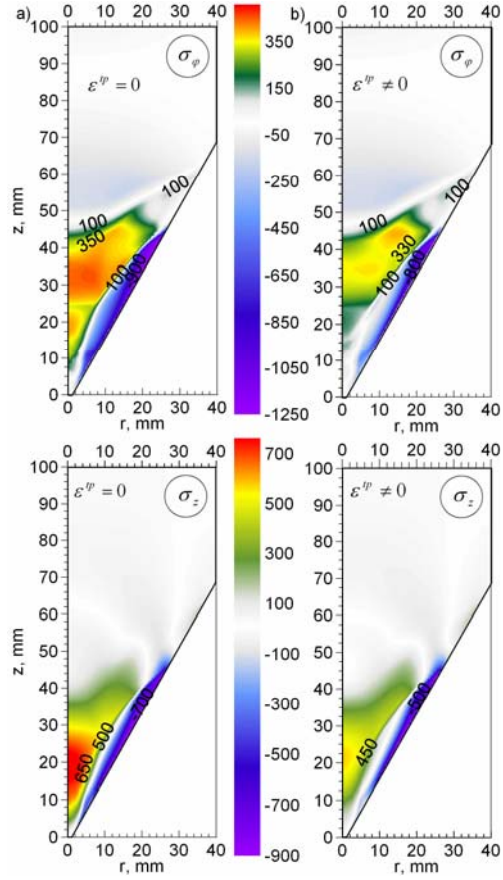

Fig. 6. Distributions of circumferential and axial stresses: without a) and with b) transformations plasticity

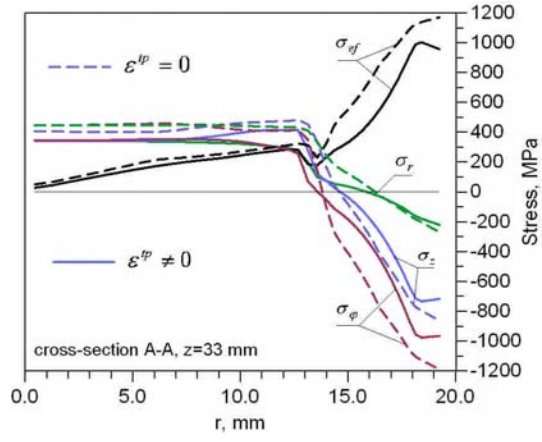

Fig. 7. Distributions of residual stresses along radius (cross section A-A)

5. Conclusions

The hardened area after cooling appeared very beneficial, as well, which means that it is very well situated. The structure of

the area after hardening is very good (certain fraction of bainite and significant fraction of martensite) (Fig. 4). In the hardened zone a small fraction of residual austenite (approximately 5%) was received [17]. The point of the lathe was not hardened at all. It is very valuable from the practical point of view with respect to the purpose of such a machinery part.

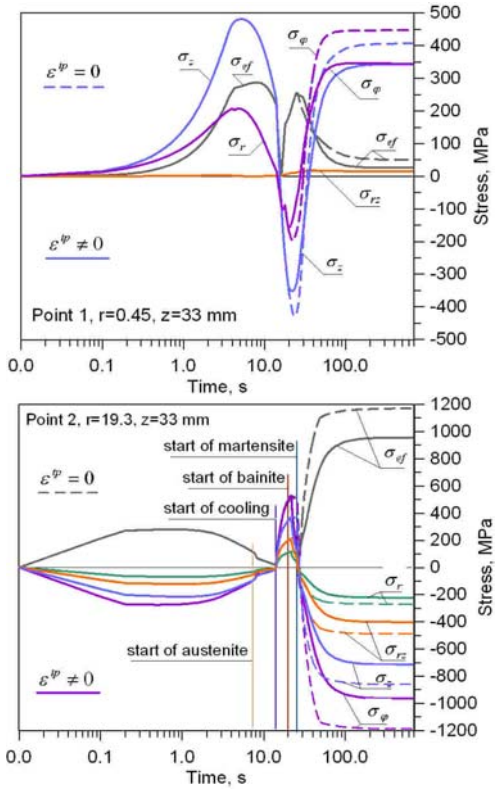

Fig. 8. History of temporary stresses in distinguished points of the cross section A-A

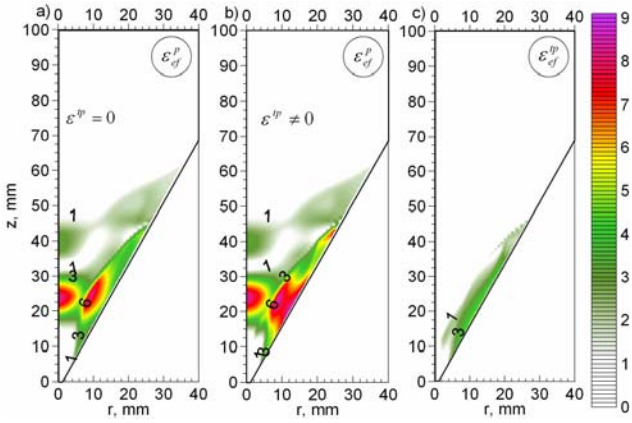

Fig. 9. Distributions of effective plastic strains and transformations plasticity ($\times 10^3$): without a) and with b) transformations plasticity, c) transformations plasticity

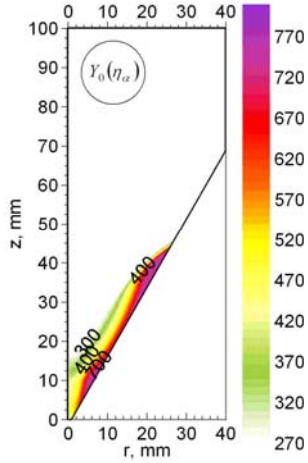

Fig. 10. Distributions of the yield point after quenching

Distribution of stresses after such hardening is beneficial. Accumulation of stresses is observed only in the zone undergoing hardening and normal stresses are negative in the subsurface layer (Figs 5-7). There are almost no stresses in the lathe core and point (see Figs 5 and 6). Influence of transformation plasticity is noticeable (see Fig. 7) but is insignificant since it is subsurface hardening. However, taking into account structural strain is very significant for mechanical phenomena. It is presented in the figure displaying the history of instantaneous stresses in the highlighted points of the section A-A (Fig. 8). The plastic strain zone is beneficial since it was created in the working part of the lat he (Fig. 9). Yet, plastic and transformation strain are not high. Increased yield point received in the hardened zone (working part of the lathe) is also valuable (Fig. 10). It indicates increased hardness of the subsurface layers of this part of the heavy duty fang lathe undergoing hardening.

References

[1] S-H. Kang, Y.T. Im, Finite element investigation of multi-phase transformation within carburized carbon steel. Journal of Materials Processing Technology 183, (2007) 241-248.

[2] S-H. Kang, Y.T. Im, Three-dimensional thermo-elestic-plastic finite element modeling of quenching process of plain carbon steel in couole with phase transformation. Journal of Materials Processing Technology 192-193, (2007) 381-390.

[3] W.P Oliveira, M.A. Savi, P.M.C.L. Pacheco, L.F.G. Souza, Thermomechanical analysis of steel cylinders with diffusional and non-diffusional phase transformations. Mechanics of Materials 42 (2010) 31-43.

[4] M. Coret, A. Combescure, A mesomodel for the numerical simulation of the multiphasic behavior of materials under anisothermal loading (application to two low-carbon steels), International Journal of Mechanical Sciences, 44, (2002) 1947-1963.

[5] S.H. Kang, Y.T. Im, Thermo-elesto-plastic finite element analysis of quenching process of carbon steel. International Journal of Mechanical Sciences 49, (2007) 13-16.

[6] A. Bokota, T. Domański, Numerical analysis of thermo-mechanical phenomena of hardening process of elements made of carbon steel C80U, Archives of Metallurgy and Materials Issue 2, vol. 52, (2007) 277-288.
[7] M. Białecki, Characteristic of steels, series F, tom I, Silesia Editor, (1987) 108-129, 155-179, (in polish).
[8] L. Taleb, F. Sidoroff, A micromechanical modelling of the Greenwood-Johnson mechanism in transformation induced plasticity, International Journal of Plasticity, 19, (2003) 1821-1842.
[9] E.P. Silva, P.M.C.L. Pacheco, M.A. Savi, On the thermo-mechanical coupling in austenite-martensite phase transformation related to the quenching process, International Journal of Solids and Structures, 41, (2004) 1139-1155.
[10] M. Suliga, Z. Muskalski, The influence of single draft on TRIP effect and mechanical propertiesof 0.09C-1.57Mn-0.9Si steel wires. Archives of Metallurgy and Materials, Issue 3, vol. 54, (2009) 677-684.
[11] M. Cherkaoui, M. Berveiller, H. Sabar, Micromechanical modeling of martensitic transformation induced plasticity (TRIP) in austenitic single crystals, International Journal of Plasticity, vol 14, no. 7, (1998) 597-626.
[12] O.C. Zienkiewicz, R.L. Taylor, The finite element method, Butterworth-Heinemann, Fifth edition, vol. 1,2 (2000).
[13] B. Raniecki, A. Bokota, S. Iskierka, R. Parkitny, Problem of Determination of Transient and Residual Stresses in a Cylinder under Progressive Induction Hardening. Proceedings of 3rd International Conference On Quenching And Control Of Distortion. Published by ASM International, (1999) 473-484.
[14] S. Serejzadeh, Modeling of temperature history and phase transformation during cooling of steel, Journal of Processing Technology, 146, (2004) 311-317.
[15] L. Huiping, Z. Guoqun, N. Shanting, H. Chuanzhen, FEM simulation of quenching process and experimental verification of simulation results, Material Science and Engineering A 452-453, (2007) 705-714.
[16] D.Y. Ju, W.M. Zhang, Y. Zhang, Modeling and experimental verification of martensitic transformation plastic behavior in carbon steel for quenching process, Material Science and Engineering A 438-440, (2006) 246-250.
[17] T. Domański, A. Bokota, A numerical model to predict microstructure of heat treated of steel element. Archives of Foundry Engineering, Vol 11,. Issue x, (2011), xx-xx (in printed).
[18] A. Bokota, S. Iskierka, Numerical analysis of phase transformation and residual stresses in steel cone-shaped elements hardened by induction and flame methods. International Journal of Mechanical Sciences, 40 (6) (1998) 617-629.
[19] M. Coret, S. Calloch, A. Combescure, Experimental study of the phase transformation plasticity of 16MND5 low carbon steel induced by proportional and nonproportional biaxial loading paths. European Journal of Mechanics A/Solids 23, (2004) 823-842.
[20] J. Jasiński, Influence of fluidized bed on diffusional processes of saturation of steel surface layer. Seria: Inżynieria Materiałowa Nr 6, Editor WIPMiFS, Częstochowa (2003), (in polish).

Analiza numeryczna pól naprężeń generowanych procesem hartowania

Streszczenie

W pracy przedstawiono model numeryczny procesu hartowania stali narzędziowej, w którym uwzględniono zjawiska mechaniczne generowane zjawiskami cieplnymi i przemianami fazowymi. W modelu zjawisk mechanicznych uwzględniono oprócz odkształceń termicznych, plastycznych i strukturalnych - również odkształcenia transformacyjne. Pola naprężeń i odkształceń uzyskuje się z rozwiązania metodą elementów skończonych równań równowagi w formie prędkościowej. Stałe termofizyczne występujące w związkach konstytutywnych uzależniono od temperatury i składu fazowego. Do wyznaczania odkształceń plastycznych wykorzystano warunek Hubera-Misesa ze wzmocnieniem izotropowym, natomiast do wyznaczania odkształceń transformacyjnych zastosowano zmodyfikowany model Leblonda. W celu oceny jakości i przydatności prezentowanego modelu dokonano analizy numerycznej pól temperatury, udziałów fazowych, naprężeń i odkształceń towarzyszących procesowi hartowania kła tokarki ze stali narzędziowej.